Physics Letters B 757 (2016) 199–206

Contents lists available at ScienceDirect

Physics Letters B

www.elsevier.com/locate/physletb

Measurement of spin correlation between top and antitop quarks produced in $p\bar{p}$ collisions at $\sqrt{s} = 1.96$ TeV

D0 Collaboration [1]

V.M. Abazov [af], B. Abbott [bp], B.S. Acharya [z], M. Adams [au], T. Adams [as], J.P. Agnew [ap], G.D. Alexeev [af], G. Alkhazov [aj], A. Alton [be,2], A. Askew [as], S. Atkins [bc], K. Augsten [g], V. Aushev [am], Y. Aushev [am], C. Avila [e], F. Badaud [j], L. Bagby [at], B. Baldin [at], D.V. Bandurin [bw], S. Banerjee [z], E. Barberis [bd], P. Baringer [bb], J.F. Bartlett [at], U. Bassler [o], V. Bazterra [au], A. Bean [bb], M. Begalli [b], L. Bellantoni [at], S.B. Beri [x], G. Bernardi [n], R. Bernhard [t], I. Bertram [an], M. Besançon [o], R. Beuselinck [ao], P.C. Bhat [at], S. Bhatia [bg], V. Bhatnagar [x], G. Blazey [av], S. Blessing [as], K. Bloom [bh], A. Boehnlein [at], D. Boline [bm], E.E. Boos [ah], G. Borissov [an], M. Borysova [am,13], A. Brandt [bt], O. Brandt [u], R. Brock [bf], A. Bross [at], D. Brown [n], X.B. Bu [at], M. Buehler [at], V. Buescher [v], V. Bunichev [ah], S. Burdin [an,3], C.P. Buszello [al], E. Camacho-Pérez [ac], B.C.K. Casey [at], H. Castilla-Valdez [ac], S. Caughron [bf], S. Chakrabarti [bm], K.M. Chan [az], A. Chandra [bv], E. Chapon [o], G. Chen [bb], S.W. Cho [ab], S. Choi [ab], B. Choudhary [y], S. Cihangir [at], D. Claes [bh], J. Clutter [bb], M. Cooke [at,12], W.E. Cooper [at], M. Corcoran [bv], F. Couderc [o], M.-C. Cousinou [l], J. Cuth [v], D. Cutts [bs], A. Das [bu], G. Davies [ao], S.J. de Jong [ad,ae], E. De La Cruz-Burelo [ac], F. Déliot [o], R. Demina [bl], D. Denisov [at], S.P. Denisov [ai], S. Desai [at], C. Deterre [ap,4], K. DeVaughan [bh], H.T. Diehl [at], M. Diesburg [at], P.F. Ding [ap], A. Dominguez [bh], A. Dubey [y], L.V. Dudko [ah], A. Duperrin [l], S. Dutt [x], M. Eads [av], D. Edmunds [bf], J. Ellison [ar], V.D. Elvira [at], Y. Enari [n], H. Evans [ax], A. Evdokimov [au], V.N. Evdokimov [ai], A. Fauré [o], L. Feng [av], T. Ferbel [bl], F. Fiedler [v], F. Filthaut [ad,ae], W. Fisher [bf], H.E. Fisk [at], M. Fortner [av], H. Fox [an], J. Franc [g], S. Fuess [at], P.H. Garbincius [at], A. Garcia-Bellido [bl], J.A. García-González [ac], V. Gavrilov [ag], W. Geng [l,bf], C.E. Gerber [au], Y. Gershtein [bi], G. Ginther [at], O. Gogota [am], G. Golovanov [af], P.D. Grannis [bm], S. Greder [p], H. Greenlee [at], G. Grenier [q,r], Ph. Gris [j], J.-F. Grivaz [m], A. Grohsjean [o,4], S. Grünendahl [at], M.W. Grünewald [aa], T. Guillemin [m], G. Gutierrez [at], P. Gutierrez [bp], J. Haley [bq], L. Han [d], K. Harder [ap], A. Harel [bl], J.M. Hauptman [ba], J. Hays [ao], T. Head [ap], T. Hebbeker [s], D. Hedin [av], H. Hegab [bq], A.P. Heinson [ar], U. Heintz [bs], C. Hensel [a], I. Heredia-De La Cruz [ac,5], K. Herner [at], G. Hesketh [ap,7], M.D. Hildreth [az], R. Hirosky [bw], T. Hoang [as], J.D. Hobbs [bm], B. Hoeneisen [i], J. Hogan [bv], M. Hohlfeld [v], J.L. Holzbauer [bg], I. Howley [bt], Z. Hubacek [g,o], V. Hynek [g], I. Iashvili [bk], Y. Ilchenko [bu], R. Illingworth [at], A.S. Ito [at], S. Jabeen [at,14], M. Jaffré [m], A. Jayasinghe [bp], M.S. Jeong [ab], R. Jesik [ao], P. Jiang [d,‡], K. Johns [aq], E. Johnson [bf], M. Johnson [at], A. Jonckheere [at], P. Jonsson [ao], J. Joshi [ar], A.W. Jung [at,16], A. Juste [ak], E. Kajfasz [l], O. Karacheban [am], D. Karmanov [ah], I. Katsanos [bh], M. Kaur [x], R. Kehoe [bu], S. Kermiche [l], N. Khalatyan [at], A. Khanov [bq], A. Kharchilava [bk], Y.N. Kharzheev [af], I. Kiselevich [ag], J.M. Kohli [x], A.V. Kozelov [ai], J. Kraus [bg], A. Kumar [bk], A. Kupco [h], T. Kurča [q,r], V.A. Kuzmin [ah], S. Lammers [ax], P. Lebrun [q,r], H.S. Lee [ab], S.W. Lee [ba], W.M. Lee [at], X. Lei [aq], J. Lellouch [n], D. Li [n], H. Li [bw], L. Li [ar], Q.Z. Li [at], J.K. Lim [ab], D. Lincoln [at], J. Linnemann [bf], V.V. Lipaev [ai], R. Lipton [at], H. Liu [bu], Y. Liu [d], A. Lobodenko [aj], M. Lokajicek [h],

http://dx.doi.org/10.1016/j.physletb.2016.03.053

R. Lopes de Sa [at], R. Luna-Garcia [ac,8], A.L. Lyon [at], A.K.A. Maciel [a], R. Madar [t], R. Magaña-Villalba [ac], S. Malik [bh], V.L. Malyshev [af], J. Mansour [u], J. Martínez-Ortega [ac], R. McCarthy [bm], C.L. McGivern [ap], M.M. Meijer [ad,ae], A. Melnitchouk [at], D. Menezes [av], P.G. Mercadante [c], M. Merkin [ah], A. Meyer [s], J. Meyer [u,10], F. Miconi [p], N.K. Mondal [z], M. Mulhearn [bw], E. Nagy [l], M. Narain [bs], R. Nayyar [aq], H.A. Neal [be], J.P. Negret [e], P. Neustroev [aj], H.T. Nguyen [bw], T. Nunnemann [w], J. Orduna [bv], N. Osman [l], J. Osta [az], A. Pal [bt], N. Parashar [ay], V. Parihar [bs], S.K. Park [ab], R. Partridge [bs,6], N. Parua [ax], A. Patwa [bn,11], B. Penning [ao], M. Perfilov [ah], Y. Peters [ap], K. Petridis [ap], G. Petrillo [bl], P. Pétroff [m], M.-A. Pleier [bn], V.M. Podstavkov [at], A.V. Popov [ai], M. Prewitt [bv], D. Price [ap], N. Prokopenko [ai], J. Qian [be], A. Quadt [u], B. Quinn [bg], P.N. Ratoff [an], I. Razumov [ai], I. Ripp-Baudot [p], F. Rizatdinova [bq], M. Rominsky [at], A. Ross [an], C. Royon [h], P. Rubinov [at], R. Ruchti [az], G. Sajot [k], A. Sánchez-Hernández [ac], M.P. Sanders [w], A.S. Santos [a,9], G. Savage [at], M. Savitskyi [am], L. Sawyer [bc], T. Scanlon [ao], R.D. Schamberger [bm], Y. Scheglov [aj], H. Schellman [aw,br], M. Schott [v], C. Schwanenberger [ap], R. Schwienhorst [bf], J. Sekaric [bb], H. Severini [bp], E. Shabalina [u], V. Shary [o], S. Shaw [ap], A.A. Shchukin [ai], V. Simak [g], P. Skubic [bp], P. Slattery [bl], D. Smirnov [az], G.R. Snow [bh], J. Snow [bo], S. Snyder [bn], S. Söldner-Rembold [ap], L. Sonnenschein [s], K. Soustruznik [f], J. Stark [k], N. Stefaniuk [am], D.A. Stoyanova [ai], M. Strauss [bp], L. Suter [ap], P. Svoisky [bw], M. Titov [o], V.V. Tokmenin [af], Y.-T. Tsai [bl], D. Tsybychev [bm], B. Tuchming [o], C. Tully [bj], L. Uvarov [aj], S. Uvarov [aj], S. Uzunyan [av], R. Van Kooten [ax], W.M. van Leeuwen [ad], N. Varelas [au], E.W. Varnes [aq], I.A. Vasilyev [ai], A.Y. Verkheev [af], L.S. Vertogradov [af], M. Verzocchi [at], M. Vesterinen [ap], D. Vilanova [o], P. Vokac [g], H.D. Wahl [as], M.H.L.S. Wang [at], J. Warchol [az], G. Watts [bx], M. Wayne [az], J. Weichert [v], L. Welty-Rieger [aw], M.R.J. Williams [ax,15], G.W. Wilson [bb], M. Wobisch [bc], D.R. Wood [bd], T.R. Wyatt [ap], Y. Xie [at], R. Yamada [at], S. Yang [d], T. Yasuda [at], Y.A. Yatsunenko [af], W. Ye [bm], Z. Ye [at], H. Yin [at], K. Yip [bn], S.W. Youn [at], J.M. Yu [be], J. Zennamo [bk], T.G. Zhao [ap], B. Zhou [be], J. Zhu [be], M. Zielinski [bl], D. Zieminska [ax], L. Zivkovic [n]

[a] *LAFEX, Centro Brasileiro de Pesquisas Físicas, Rio de Janeiro, Brazil*
[b] *Universidade do Estado do Rio de Janeiro, Rio de Janeiro, Brazil*
[c] *Universidade Federal do ABC, Santo André, Brazil*
[d] *University of Science and Technology of China, Hefei, People's Republic of China*
[e] *Universidad de los Andes, Bogotá, Colombia*
[f] *Charles University, Faculty of Mathematics and Physics, Center for Particle Physics, Prague, Czech Republic*
[g] *Czech Technical University in Prague, Prague, Czech Republic*
[h] *Institute of Physics, Academy of Sciences of the Czech Republic, Prague, Czech Republic*
[i] *Universidad San Francisco de Quito, Quito, Ecuador*
[j] *LPC, Université Blaise Pascal, CNRS/IN2P3, Clermont, France*
[k] *LPSC, Université Joseph Fourier Grenoble 1, CNRS/IN2P3, Institut National Polytechnique de Grenoble, Grenoble, France*
[l] *CPPM, Aix-Marseille Université, CNRS/IN2P3, Marseille, France*
[m] *LAL, Univ. Paris-Sud, CNRS/IN2P3, Université Paris-Saclay, Orsay, France*
[n] *LPNHE, Universités Paris VI and VII, CNRS/IN2P3, Paris, France*
[o] *CEA, Irfu, SPP, Saclay, France*
[p] *IPHC, Université de Strasbourg, CNRS/IN2P3, Strasbourg, France*
[q] *IPNL, Université Lyon 1, CNRS/IN2P3, Villeurbanne, France*
[r] *Université de Lyon, Lyon, France*
[s] *III. Physikalisches Institut A, RWTH Aachen University, Aachen, Germany*
[t] *Physikalisches Institut, Universität Freiburg, Freiburg, Germany*
[u] *II. Physikalisches Institut, Georg-August-Universität Göttingen, Göttingen, Germany*
[v] *Institut für Physik, Universität Mainz, Mainz, Germany*
[w] *Ludwig-Maximilians-Universität München, München, Germany*
[x] *Panjab University, Chandigarh, India*
[y] *Delhi University, Delhi, India*
[z] *Tata Institute of Fundamental Research, Mumbai, India*
[aa] *University College Dublin, Dublin, Ireland*
[ab] *Korea Detector Laboratory, Korea University, Seoul, Republic of Korea*
[ac] *CINVESTAV, Mexico City, Mexico*
[ad] *Nikhef, Science Park, Amsterdam, The Netherlands*
[ae] *Radboud University Nijmegen, Nijmegen, The Netherlands*
[af] *Joint Institute for Nuclear Research, Dubna, Russia*
[ag] *Institute for Theoretical and Experimental Physics, Moscow, Russia*
[ah] *Moscow State University, Moscow, Russia*
[ai] *Institute for High Energy Physics, Protvino, Russia*
[aj] *Petersburg Nuclear Physics Institute, St. Petersburg, Russia*
[ak] *Institució Catalana de Recerca i Estudis Avançats (ICREA) and Institut de Física d'Altes Energies (IFAE), Barcelona, Spain*

[al] Uppsala University, Uppsala, Sweden
[am] Taras Shevchenko National University of Kyiv, Kiev, Ukraine
[an] Lancaster University, Lancaster LA1 4YB, United Kingdom
[ao] Imperial College London, London SW7 2AZ, United Kingdom
[ap] The University of Manchester, Manchester M13 9PL, United Kingdom
[aq] University of Arizona, Tucson, AZ 85721, USA
[ar] University of California Riverside, Riverside, CA 92521, USA
[as] Florida State University, Tallahassee, FL 32306, USA
[at] Fermi National Accelerator Laboratory, Batavia, IL 60510, USA
[au] University of Illinois at Chicago, Chicago, IL 60607, USA
[av] Northern Illinois University, DeKalb, IL 60115, USA
[aw] Northwestern University, Evanston, IL 60208, USA
[ax] Indiana University, Bloomington, IN 47405, USA
[ay] Purdue University Calumet, Hammond, IN 46323, USA
[az] University of Notre Dame, Notre Dame, IN 46556, USA
[ba] Iowa State University, Ames, IA 50011, USA
[bb] University of Kansas, Lawrence, KS 66045, USA
[bc] Louisiana Tech University, Ruston, LA 71272, USA
[bd] Northeastern University, Boston, MA 02115, USA
[be] University of Michigan, Ann Arbor, MI 48109, USA
[bf] Michigan State University, East Lansing, MI 48824, USA
[bg] University of Mississippi, University, MS 38677, USA
[bh] University of Nebraska, Lincoln, NE 68588, USA
[bi] Rutgers University, Piscataway, NJ 08855, USA
[bj] Princeton University, Princeton, NJ 08544, USA
[bk] State University of New York, Buffalo, NY 14260, USA
[bl] University of Rochester, Rochester, NY 14627, USA
[bm] State University of New York, Stony Brook, NY 11794, USA
[bn] Brookhaven National Laboratory, Upton, NY 11973, USA
[bo] Langston University, Langston, OK 73050, USA
[bp] University of Oklahoma, Norman, OK 73019, USA
[bq] Oklahoma State University, Stillwater, OK 74078, USA
[br] Oregon State University, Corvallis, OR 97331, USA
[bs] Brown University, Providence, RI 02912, USA
[bt] University of Texas, Arlington, TX 76019, USA
[bu] Southern Methodist University, Dallas, TX 75275, USA
[bv] Rice University, Houston, TX 77005, USA
[bw] University of Virginia, Charlottesville, VA 22904, USA
[bx] University of Washington, Seattle, WA 98195, USA

ARTICLE INFO

Article history:
Received 31 December 2015
Received in revised form 24 February 2016
Accepted 18 March 2016
Available online 25 March 2016
Editor: M. Doser

ABSTRACT

We present a measurement of the correlation between the spins of t and $\bar{t}$ quarks produced in proton–antiproton collisions at the Tevatron Collider at a center-of-mass energy of 1.96 TeV. We apply a matrix element technique to dilepton and single-lepton+jets final states in data accumulated with the D0 detector that correspond to an integrated luminosity of 9.7 fb^{-1}. The measured value of the correlation coefficient in the off-diagonal basis, $O_{\text{off}} = 0.89 \pm 0.22$ (stat + syst), is in agreement with the standard model prediction, and represents evidence for a top–antitop quark spin correlation difference from zero at a level of 4.2 standard deviations.

E-mail address: Viatcheslav.Sharyy@cea.fr (V. Shary).
[1] with visitors from:
[2] Augustana College, Sioux Falls, SD, USA.
[3] The University of Liverpool, Liverpool, UK.
[4] DESY, Hamburg, Germany.
[5] CONACyT, Mexico City, Mexico.
[6] SLAC, Menlo Park, CA, USA.
[7] University College London, London, UK.
[8] Centro de Investigacion en Computacion – IPN, Mexico City, Mexico.
[9] Universidade Estadual Paulista, São Paulo, Brazil.
[10] Karlsruher Institut für Technologie (KIT) – Steinbuch Centre for Computing (SCC), D-76128 Karlsruhe, Germany.
[11] Office of Science, U.S. Department of Energy, Washington, D.C. 20585, USA.
[12] American Association for the Advancement of Science, Washington, D.C. 20005, USA.
[13] Kiev Institute for Nuclear Research, Kiev, Ukraine.
[14] University of Maryland, College Park, MD 20742, USA.
[15] European Organization for Nuclear Research (CERN), Geneva, Switzerland.
[16] Purdue University, West Lafayette, IN 47907, USA.
[‡] Deceased.

1. Introduction

The top quark is the heaviest elementary particle in the standard model (SM) [1–4]. Despite the fact that the top quark decays weakly, its large mass leads to a very short lifetime of $\approx 5 \cdot 10^{-25}$ s [5–7]. It decays to a W boson and a b quark before hadronizing, a process that has a characteristic time of $1/\Lambda_{\text{QCD}} \approx (200\ \text{MeV})^{-1}$ equivalent to $\tau_{\text{had}} \approx 3.3 \cdot 10^{-24}$ s, where Λ_{QCD} is the fundamental scale of quantum chromodynamics (QCD). The top quark lifetime is also smaller than the spin-decorrelation time from spin–spin interactions with the light quarks generated in the fragmentation process [8], $\tau_{\text{spin}} \approx m_t/\Lambda^2_{\text{QCD}} \approx (0.2\ \text{MeV})^{-1} \approx 3 \cdot 10^{-21}$ s [9]. The top quark thus provides a unique opportunity to measure spin-related phenomena in the quark sector by exploiting kinematic properties of its decay products.

In proton–antiproton ($p\bar{p}$) collisions, the dominant process for producing top quarks is through top–antitop ($t\bar{t}$) quark pairs. This QCD process yields unpolarized t and $\bar{t}$ quarks, but leaves the spins

of t and $\bar{t}$ correlated. A spin correlation observable can be defined as [10]

$$O_{ab} = \langle 4(S_t \cdot \hat{a})(S_{\bar{t}} \cdot \hat{b})\rangle = \frac{\sigma(\uparrow\uparrow) + \sigma(\downarrow\downarrow) - \sigma(\uparrow\downarrow) - \sigma(\downarrow\uparrow)}{\sigma(\uparrow\uparrow) + \sigma(\downarrow\downarrow) + \sigma(\uparrow\downarrow) + \sigma(\downarrow\uparrow)},$$

where S is a spin operator, $\hat{a}$, $\hat{b}$ are the spin quantization axes for the top quark ($\hat{a}$) and the antitop quark ($\hat{b}$), $\langle\rangle$ refers to an expectation value, σ is the $t\bar{t}$ production cross section, and the arrows refer to the spin states of the t and $\bar{t}$ quarks relative to the $\hat{a}$ and $\hat{b}$ axes. The strength of the correlation depends on the $t\bar{t}$ production mechanism [11–13]. In $p\bar{p}$ collisions at a center-of-mass energy of 1.96 TeV, the correlation of spins is predicted to be $O_{\rm off} = 0.80^{+0.01}_{-0.02}$ [10] in the off-diagonal spin basis, the basis in which the strength of the spin correlation is maximal at the Tevatron [12]. The most significant contribution is from the quark–antiquark annihilation process ($q\bar{q} \to t\bar{t}$) with a spin correlation strength of ≈ 0.99, while the gluon–gluon (gg) fusion process ($gg \to t\bar{t}$) has anticorrelated spins with a typical strength of ≈ -0.36 at next-to-leading order (NLO) in QCD [10,14,15]. Contributions to $t\bar{t}$ production from beyond the SM can have different dynamics that affect the strength of the $t\bar{t}$ spin correlation.

Evidence for $t\bar{t}$ spin correlations based on a matrix element technique [16], was presented by the D0 collaboration. Earlier lower precision measurements used a template method [17,18]. Spin correlation effects have also been measured in proton–proton (pp) collisions by two LHC collaborations, ATLAS and CMS, at a center-of-mass energy of 7 TeV [19–22] and at 8 TeV [23,24]. The main mechanism for $t\bar{t}$ production at the LHC is the gg fusion process. The spin correlation at the LHC arises mainly from the fusion of like-helicity gluons [25]. The differences between pp and $p\bar{p}$ incident channels, the different sources of spin correlation (quark–antiquark annihilation versus like-helicity gg fusion), and their different collision energies, make the measurements of the strength of the spin correlation at both the Tevatron and LHC interesting and complementary.

In this letter, we present an updated measurement of the $t\bar{t}$ spin correlation strength in $p\bar{p}$ collisions at $\sqrt{s} = 1.96$ TeV. The measurement uses the statistics accumulated during 2001–2011 data taking period of the Fermilab Tevatron Collider, which corresponds to an integrated luminosity of 9.7 fb^{-1}, which is almost two times more than in our previous publication [16].

2. Detector, event selection and simulation, background

The D0 detector is described in Refs. [26–32]. It has a central tracking system consisting of a silicon microstrip tracker and a central fiber tracker, both located within an ~ 2 T superconducting solenoidal magnet. The central tracking system is designed to optimize tracking and vertexing at detector pseudorapidities of $|\eta_{\rm det}| < 2.5$.[1] The liquid-argon sampling calorimeter has a central section covering pseudorapidities $|\eta_{\rm det}|$ up to ≈ 1.1, and two end calorimeters that extend coverage to $|\eta_{\rm det}| \approx 4.2$, with all three housed in separate cryostats. A outer muon system, with pseudorapidity coverage of $|\eta_{\rm det}| < 2$, consists of a layer of tracking detectors and scintillation trigger counters in front of 1.8 T iron toroids, followed by two similar layers after the toroids.

Within the SM, the top quark decays with almost 100% probability into a W boson and a b quark. We also include two final states: the dilepton final state ($\ell\ell$), where both W bosons decay to leptons, and the lepton+jets final state (ℓ+jets), where one of the W bosons decays into a pair of quarks and one decays to a lepton and a neutrino. The ℓ+jets and $\ell\ell$ final states contain, respectively, one or two isolated charged leptons. In both final states we consider only electrons and muons, including those from τ-lepton decay, $W \to \tau\nu_\tau \to \ell\nu_\ell\nu_\tau$. We also require the presence of two b quark jets, two light-quark jets from W decay (in ℓ+jets), and a significant missing transverse momentum ($\not\!\!p_T$) due to the escaping neutrinos.

We use the following selection criteria. In the $\ell\ell$ channels, we require two isolated leptons with $p_T > 15$ GeV, both originating from the same $p\bar{p}$ interaction vertex. The ℓ+jets channels require one isolated lepton with $p_T > 20$ GeV. We consider electrons and muons identified using the standard D0 criteria [33,34], in the pseudorapidity range of $|\eta_{\rm det}| < 2.0$ for muons, and $|\eta_{\rm det}| < 1.1$ for electrons. In the $\ell\ell$ channels, we consider in addition forward electrons in the range of $1.5 < |\eta_{\rm det}| < 2.5$. Jets are reconstructed and identified from energy deposition in the calorimeter using an iterative midpoint cone algorithm [35] of radius $\sqrt{(\Delta\phi)^2 + (\Delta\eta)^2} = 0.5$. Their energies are corrected using the jet energy scale (JES) algorithm [36]. All $\ell\ell$ channels also require the presence of at least two jets with $p_T > 20$ GeV and $|\eta_{\rm det}| < 2.5$. For the ℓ+jets final state, at least four jets must be identified with the same p_T and $\eta_{\rm det}$ cutoffs, but with the leading jet required to have $p_T > 40$ GeV. When a muon track is found within a jet cone, the JES calculation takes that muon momentum into account, assuming that the muon originates from the semileptonic decay of a heavy-flavor hadron belonging to the jet. To identify b quark jets, we use a multivariate b quark jet identification discriminant that combines information from the impact parameters of the tracks and variables that characterize the presence and properties of secondary vertices within the jet [37]. We require that at least one jet is identified as a b quark jet in the $\ell\ell$ channels, and at least two such jets in the ℓ+jets channels. To improve signal purity, additional selections based on the global event topology are applied [38,39] in each final state. A detailed description of event selection can be found in Ref. [38] for the $\ell\ell$ and in Ref. [39] for the ℓ+jets final states.

To simulate $t\bar{t}$ events we use the next-to-leading (NLO) order Monte Carlo (MC) QCD generator MC@NLO (version 3.4) [40,41], interfaced to HERWIG (version 6.510) [42] for parton showering and hadronization. The CTEQ6M parton distribution functions (PDF) [43,44] are used to generate events at a top quark mass of $m_t = 172.5$ GeV. We use two samples, one including spin correlation effects, and the other without correlation. The generated events are processed through a GEANT3-based [45] simulation of the D0 detector. To simulate effects from additional overlapping $p\bar{p}$ interactions, "zero bias" events taken from collider data with an unbiassed trigger based solely on beam bunch crossings are overlaid on the simulated events. Simulated events are then processed with the same reconstruction program as data.

In the $\ell\ell$ channels, the main sources of background are Drell–Yan production, $q\bar{q} \to Z/\gamma^\star \to \ell\ell$, diboson WW, WZ, ZZ production, and instrumental background. The instrumental background arises mainly from multijet and $(W \to \ell\nu)$+jets events, in which one jet in W+jets or two jets in multijet events are misidentified as electrons, or where muons or electrons originating from semileptonic decay of heavy-flavor hadrons appear to be isolated. The instrumental background is determined from data, while the other backgrounds are estimated using MC simulations. For the ℓ+jets channel, in addition to the Drell–Yan and diboson production, the contribution from W+jets production is estimated from MC simulation, but normalized to data. Electroweak single top quark production and $t\bar{t}$ dilepton final states are also considered as background. The Drell–Yan and $(W \to \ell\nu)$+jets samples

[1] The pseudorapidity is defined as $\eta = -\ln[\tan(\theta/2)]$, where θ is the polar angle of the reconstructed particle originating from the $p\bar{p}$ collision vertex, relative to the proton beam direction. Detector pseudorapidity $\eta_{\rm det}$ is defined relative to the center of the detector.

Table 1
Numbers of expected events, and numbers of events found in data.

	$Z/\gamma^\star$	Instrumental	Diboson	$t\bar{t}$	Total	Data
$e\mu$	13.2	16.4	3.7	303.4	336.7	347
ee	12.2	1.8	1.9	102.4	118.3	105
$\mu\mu$	9.8	0.0	1.7	85.0	96.5	93
	W+jets	Multijet	Other			
e+jets	22.7	23.1	15.3	427.4	488.6	534
μ+jets	24.1	3.5	11.6	341.4	380.6	440

are generated with the leading order (LO) matrix element generator ALPGEN (version v2.11) [46], interfaced to PYTHIA [47] (version 6.409, D0 modified tune A [48]) for parton showering and hadronization. Diboson events are generated with PYTHIA. More details about background estimation can be found in Refs. [38,39]. Table 1 shows the number of expected events for each background source and for the signal, and the number of selected events in data. The number of the expected $t\bar{t}$ events is normalized to the NLO cross section of $7.45^{+0.48}_{-0.67}$ pb [49]. The observed number of events in the ℓ+jets channel is higher than the expected, mainly due to an excess in the μ+jets channel. The expected and observed number of events are consistent when the systematic uncertainties, partially correlated between the ℓ+jets and $\ell\ell$ channels, are taken into account. These uncertainties are of the order of 10%. The most important contributions are the integrated luminosity, b-quark jet modeling, uncertainties on the $t\bar{t}$ modeling and uncertainty in the heavy flavor NLO K-factors of the W+jets background in the ℓ+jets channel.

3. Measurement technique and results

Our measurement uses the same matrix element (ME) approach as Refs. [16,50], adapted to the spin correlation measurement. This method consists of calculating the spin correlation discriminant [51]

$$R(x) = \frac{P_{t\bar{t}}(x, \mathrm{SM})}{P_{t\bar{t}}(x, \mathrm{SM}) + P_{t\bar{t}}(x, \mathrm{null})}, \quad (1)$$

where $P_{t\bar{t}}(x, \mathscr{H})$ is a per-event probability for hypothesis $\mathscr{H}$ for the vector of the reconstructed object parameters x. Hypothesis $\mathscr{H} = \mathrm{SM}$ assumes the $t\bar{t}$ spin correlation strength predicted by the SM, and $\mathscr{H} = \mathrm{null}$ assumes uncorrelated spins. These probabilities are calculated from the integral

$$P_{t\bar{t}}(x, \mathscr{H}) = \frac{1}{\sigma_{\mathrm{obs}}} \int f_{\mathrm{PDF}}(q_1) f_{\mathrm{PDF}}(q_2) \times \frac{(2\pi)^4 |\mathscr{M}(y, \mathscr{H})|^2}{q_1 q_2 s} W(x, y) d\Phi^6 dq_1 dq_2. \quad (2)$$

Here, q_1 and q_2 represent the respective fractions of proton and antiproton momentum carried by the initial state partons, f_{PDF} represents the parton distribution functions, s is the square of the $p\bar{p}$ center-of-mass energy, and y refers to partonic final state four-momenta of the particles. The detector transfer functions, $W(x, y)$, correspond to the probability to reconstruct four-momenta y as x, $d\Phi^6$ represents the six-body phase space, and σ_{obs} is the observed $t\bar{t}$ production cross section, calculated using $\mathscr{M}(\mathscr{H} = \mathrm{null})$, taking into account the efficiency of the selection. The same σ_{obs} is used for $\mathscr{H} = \mathrm{null}$ and $\mathscr{H} = \mathrm{SM}$ hypotheses, because the difference in observed cross-sections is small, at the order of percent, and affects only the separation power of the discriminant R. This calculation uses the LO matrix element $\mathscr{M}(y, \mathscr{H})$ for the processes $q\bar{q} \to t\bar{t} \to W^+W^-b\bar{b} \to \ell^\pm \nu_\ell q q' b\bar{b}$ or $\ell^+\ell^-\nu_\ell\bar{\nu}_\ell b\bar{b}$, calculated according to the spin correlation hypothesis $\mathscr{H}$. The matrix element $\mathscr{M}$ is averaged over the colors and spins of the initial partons, and summed over the final colors and spins. For the hypothesis $\mathscr{H} = \mathrm{null}$, we set the spin correlation part to zero [11,12]. In the calculation, we assume perfect measurements of the lepton and jet directions, and perfect measurement of electron energy, which reduces the number of dimensions that require integration. The probability is obtained by integrating over the remaining kinematic variables. In the $\ell\ell$ final state, we use the top and antitop quark masses, W^+ and W^- boson masses, p_T of two jets, $1/p_T$ for any muons and p_T and ϕ of the $t\bar{t}$ system as integration variables. In the ℓ+jets final state, the variables are the top and antitop quark masses, the mass of the W boson decaying to $q\bar{q}'$, p_T of the d-type quark jet, p_z of the leptonically decaying top quark and $1/p_T$ of a muon. Given the inability to know the flavor of the two quarks from the W boson decay, or which b-tagged jet originates from the decay of the top or anti-top quark, all possible jet-parton assignments are considered and $P_{t\bar{t}}$ is calculated as the sum over all the probabilities.

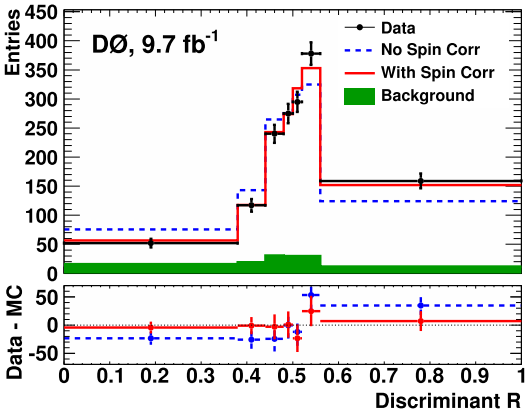

Fig. 1. Distribution of the spin correlation discriminant R in data and for the MC@NLO $t\bar{t}$ prediction with background, showing the merged results from $\ell\ell$ and ℓ+jets events. The lower plot represents the difference between data and simulation with SM spin correlation and without spin correlation. The error bars correspond to statistical uncertainties.

The distributions in the discriminant R of Eq. (1) are calculated for simulated $t\bar{t}$ events with SM spin correlation and with uncorrelated spins. These and the expected contributions from the background events are used as templates to fit the R distribution in data through a binned maximum-likelihood fit with two free parameters: the $t\bar{t}$ production cross section $\sigma_{t\bar{t}}$, and the measured fraction of events with the SM spin correlation strength, f.

This fit of the distributions in the $\ell\ell$ and ℓ+jets channels is performed simultaneously, with the expected number of events n_i in each bin i given by

$$n_i = \frac{\sigma_{t\bar{t}}}{7.45\ \mathrm{pb}} \left(f n^i_{\mathrm{SM}} + (1 - f) n^i_{\mathrm{null}} \right) + n^i_{\mathrm{bckg}}, \quad (3)$$

where n^i_{SM} and n^i_{null} are the number of events in bin i based on the MC@NLO prediction, with and without spin correlations, and n^i_{bckg} is the expected number of background events in the same bin. We use a non-uniform bin width and require a sufficiently large number of events for each bin in order to avoid bins with zero events, as they could bias the fit result. The exact number of bins and their size were optimized to give the smallest expected statistical uncertainty in the case of the SM spin correlation. We use the same number and widths of the bins for the ℓ+jets and $\ell\ell$ channels so as to keep the bin optimization procedure relatively simple. The fit yields $f = 1.16 \pm 0.21$ (stat). The R distribution for the combined $\ell\ell$ and ℓ+jets channels is shown in Fig. 1. We estimate the significance of the non-zero spin correlation hypothesis

Table 2
Systematic uncertainties (absolute values) on the spin correlation strength $O_{\rm off}^{meas}$.

Source	Uncertainty in $O_{\rm off}^{meas}$
Modeling of signal	±0.135
PDF	±0.027
Statistical fluctuations in MC	±0.026
Identification and reconstruction	±0.032
Background contribution	±0.019
Total	±0.15

using the Feldman and Cousins frequentist procedure [52], assuming that the parameter f is in the range $[0, 1]$, even though the measured value obtained in the fit is outside of the range $[0, 1]$.

To translate the f value to the spin correlation strength in the off-diagonal basis $O_{\rm off}$, we must consider the value of the spin correlation strength in the simulation $O_{\rm off}^{\rm MC}$. We choose to obtain this value in the simulated $\ell\ell$ samples from the expected value of $k_1 k_2 O_{\rm off}^{\rm MC} = -9\langle\cos\theta_1 \cdot \cos\theta_2\rangle$ [14], where θ_1 and θ_2 represent angles between the respective direction of a positively and negatively charged lepton and the spin quantization axes in the t and $\bar{t}$ rest frame. The parameters k_1 and k_2 are the spin analyzing-power coefficients of the top quark (equal to 1 for leptons at LO in QCD) [53]. With MC@NLO, the value calculated for the parton-level distributions before any selections is found to equal $O_{\rm off}^{\rm mc@nlo} = 0.766$ in the off-diagonal basis. The measured spin correlation strength for ℓ+jets and $\ell\ell$ channels is therefore

$$O_{\rm off}^{\rm meas} = O_{\rm off}^{\rm mc@nlo} \cdot f = 0.89 \pm 0.16\ (\text{stat})\ ,$$

in agreement with the NLO QCD calculation $O_{\rm off} = 0.80^{+0.01}_{-0.02}$ [10]. For events in the ℓ+jets channel, the result is

$$O_{\rm off}^{\ell+\rm jets} = 1.02 \pm 0.24\ (\text{stat})\ ,$$

and for $\ell\ell$ channel the result is

$$O_{\rm off}^{\ell\ell} = 0.80 \pm 0.22\ (\text{stat})\ .$$

We can reinterpret the measured fraction f as the related measurement of the spin correlation observable $O_{\rm spin} = \langle\frac{4}{3}(S_t \cdot S_{\bar{t}})\rangle$ [10]. This observable characterizes the distribution in the opening angle, φ, between the directions of the two leptons in dilepton events or between the lepton and the up-type quark from the W decay in ℓ+jets events, where the directions are defined in the t and $\bar{t}$ rest frame:

$$\frac{1}{\sigma}\frac{d\sigma}{d\cos\varphi} = \frac{1}{2}(1 - k_1 k_2 O_{\rm spin}\cos\varphi). \tag{4}$$

The prediction from the MC@NLO simulation is given by the expectation value $k_1 k_2 O_{\rm spin}^{\rm mc@nlo} = -3\langle\cos\varphi\rangle$ at the parton level, without any selections, and found to be $O_{\rm spin}^{\rm mc@nlo} = 0.20$. The value measured from data is therefore

$$O_{\rm spin}^{\rm meas} = O_{\rm spin}^{\rm mc@nlo} \cdot f = 0.23 \pm 0.04(\text{stat}),$$

consistent with the NLO QCD calculation of $O_{\rm spin} = 0.218 \pm 0.002$ [10].

4. Systematic uncertainties

The estimated systematic uncertainties are summarized in Table 2. These are obtained by replacing the nominal $t\bar{t}$ and background results with modified templates, refitting the data and determining the new fraction f_Δ.

We consider several sources of uncertainties in the modeling of the signal. These include initial-state and final-state radiation, the simulation of hadronization and underlying events, the effects of higher-order corrections, color-reconnection and uncertainty on the top quark mass. The details of the corresponding samples and parameters are discussed in Refs. [1,2].

For the PDF uncertainty, we change the 20 CTEQ6 eigenvectors independently and add the resulting uncertainties in quadrature. In modeling both the estimated signal and PDF uncertainties, the event samples have different fractional contributions from gg fusion and $q\bar{q}$ annihilation, and therefore different spin-correlation strengths. We take this into account by normalizing the measured fraction to the spin-correlation strength of the sample $O_{\rm off}^{\rm MC}$, in a way similar to that used for the nominal measurement $O_{\rm off}^{\Delta} = f_\Delta \cdot O_{\rm off}^{\rm MC}$.

The statistical uncertainty in MC templates is estimated using the ensemble testing technique. The new ensembles are created through a random generation of a new number of events in each bin of the MC template assuming a Gaussian distribution in the number of events in the bin. The same distribution in data is fitted with the modified templates and the dispersion in the fit results over 1000 ensembles is used as an estimation of the statistical uncertainty in the MC templates.

The uncertainty on identification and reconstruction effects includes uncertainties on lepton, jet and b tagging identification efficiencies, jet energy resolution and scale corrections, trigger efficiencies, and the luminosity. The uncertainty in the background contributions includes all uncertainties that affect the signal-to-background ratio that are not contained in the previous categories. These uncertainties include uncertainties in theoretical cross sections for backgrounds, uncertainty in Z boson p_T distribution, and uncertainties in instrumental background contributions.

The total absolute systematic uncertainty on the spin correlation observable $O_{\rm off}^{meas}$, calculated as a quadratic sum over all individual sources, is 0.15, as shown in Table 2.

5. Spin correlation and the $t\bar{t}$ production mechanism

The strength of the $t\bar{t}$ spin correlation in the SM is strongly dependent on the $t\bar{t}$ production mechanism. The spin correlation measurement thus provides a way of measuring the fraction of events produced via gg fusion, f_{gg} [13]. The f_{gg} fraction is not well defined at orders higher than LO QCD. The difficulty arises from the fact that the cross sections for the $gq \to t\bar{t}q$ and $g\bar{q} \to t\bar{t}\bar{q}$ processes at LO, as well as gg and $q\bar{q}$ production at NLO, contain a singularity when the final state quark is collinear with the quark in the initial state. This makes the integration over the phase space divergent [15,54,55]. In practice, this singularity is absorbed into the definition of the PDF, but the final results depend on the scheme used for regularization. For the NLO PDF, the $\overline{\rm MS}$ scheme is usually preferred. The gq and $g\bar{q}$ contribution at NLO is of the order of a few percent [10,14,15], and considering that the overall spin correlation strength is $\approx 80\%$, we neglect these smaller contributions, and determine f_{gg} from the relation

$$O = (1 - f_{gg})O_{q\bar{q}} + f_{gg} O_{gg}\ .$$

Assuming $O_{q\bar{q}} \approx 1$, the gluon fraction becomes

$$f_{gg} \approx \frac{1 - O}{1 - O_{gg}},$$

where O is the measured value of the total spin correlation strength, and O_{gg} is the SM value of the spin correlation strength for gg events.

The NLO calculation in the off-diagonal basis using the CT10 PDF yields $O_{gg} = -0.36 \pm 0.02$ [10,14,15]. The systematic uncertainty on the observable O can be translated to the uncertainty

on the gluon fraction that includes an additional contribution from the theoretical uncertainty on O_{gg}. In the absence of non-SM contributions, the fraction of $t\bar{t}$ events produced through gluon fusion becomes

$$f_{gg} = 0.08 \pm 0.12(\text{stat}) \pm 0.11(\text{syst}) = 0.08 \pm 0.16(\text{stat} + \text{syst}) ,$$

in agreement with the NLO prediction of $f_{gg} = 0.135$ [10,14,15].

6. Summary

We have presented an updated measurement of $t\bar{t}$ spin correlations with the D0 detector for an integrated luminosity of 9.7 fb^{-1}. The result of the measurement of the strength of the $t\bar{t}$ spin correlation in the off-diagonal basis is

$$\begin{aligned} O_{\text{off}} &= 0.89 \pm 0.16\ (\text{stat}) \pm 0.15\ (\text{syst}) \\ &= 0.89 \pm 0.22\ (\text{stat} + \text{syst}). \end{aligned}$$

This result is in agreement with the NLO QCD calculation $O_{\text{off}} = 0.80^{+0.01}_{-0.02}$ [10] and supersedes that reported in Ref. [16]. Using the Feldman and Cousins approach for interval setting [52], and assuming uncorrelated $t\bar{t}$ spins, we estimate a probability (p-value) of 2.5×10^{-5} for obtaining a spin correlation larger than the observed value. This corresponds to evidence for spin correlation in $t\bar{t}$ events at a significance of 4.2 standard deviations.

In the absence of non-SM contributions, we use the spin correlation strength measurement to constrain the fraction of events produced through gluon fusion at NLO QCD and obtain

$$f_{gg} = 0.08 \pm 0.16(\text{stat} + \text{syst}) ,$$

in good agreement with SM prediction.

Acknowledgments

We thank the staffs at Fermilab and collaborating institutions, and acknowledge support from the Department of Energy and National Science Foundation (United States of America); Alternative Energies and Atomic Energy Commission and National Center for Scientific Research/ National Institute of Nuclear and Particle Physics (France); Ministry of Education and Science of the Russian Federation, National Research Center "Kurchatov Institute" of the Russian Federation, and Russian Foundation for Basic Research (Russia); National Council for the Development of Science and Technology and Carlos Chagas Filho Foundation for the Support of Research in the State of Rio de Janeiro (Brazil); Department of Atomic Energy and Department of Science and Technology (India); Administrative Department of Science, Technology and Innovation(Colombia); National Council of Science and Technology (Mexico); National Research Foundation of Korea (Korea); Foundation for Fundamental Research on Matter (The Netherlands); Science and Technology Facilities Council and The Royal Society (United Kingdom); Ministry of Education, Youth and Sports (Czech Republic); Bundesministerium für Bildung und Forschung (Federal Ministry of Education and Research) and Deutsche Forschungsgemeinschaft (German Research Foundation) (Germany); Science Foundation Ireland (Ireland); Swedish Research Council (Sweden); China Academy of Sciences and National Natural Science Foundation of China (China); and Ministry of Education and Science of Ukraine (Ukraine).

References

[1] V.M. Abazov, et al., D0 Collaboration, Precision measurement of the top-quark mass in lepton+jets final states, Phys. Rev. Lett. 113 (2014) 032002.
[2] V.M. Abazov, et al., D0 Collaboration, Precision measurement of the top-quark mass in lepton+jets final states, Phys. Rev. D 91 (2015) 112003.
[3] CDF Collaboration, D0 Collaboration, Combination of CDF and D0 results on the mass of the top quark using up to 9.7 fb^{-1} at the Tevatron, arXiv:1407.2682, 2014.
[4] ATLAS Collaboration, CDF Collaboration, CMS Collaboration, and D0 Collaboration, First combination of Tevatron and LHC measurements of the top-quark mass, arXiv:1403.4427, 2014.
[5] M. Jezabek, J.H. Kühn, Semileptonic decays of top quarks, Phys. Lett. B 207 (1988) 91.
[6] M. Jezabek, J.H. Kühn, QCD corrections to semileptonic decays of heavy quarks, Nucl. Phys. 314 (1989) 1.
[7] V.M. Abazov, et al., D0 Collaboration, An improved determination of the width of the top quark, Phys. Rev. D 85 (2012) 091104.
[8] A.F. Falk, M.E. Peskin, Production, decay, and polarization of excited heavy hadrons, Phys. Rev. D 49 (1994) 3320.
[9] S. Willenbrock, The standard model and the top quark, NATO Sci. Ser. II 123 (2003) 1.
[10] W. Bernreuther, Z.-G. Si, Distributions and correlations for top quark pair production and decay at the Tevatron and LHC, Nucl. Phys. 837 (2010) 90.
[11] G. Mahlon, S.J. Parke, Angular correlations in top quark pair production and decay at hadron colliders, Phys. Rev. D 53 (1996) 4886.
[12] G. Mahlon, S.J. Parke, Maximizing spin correlations in top quark pair production at the Tevatron, Phys. Lett. B 411 (1997) 173.
[13] W. Bernreuther, A. Brandenburg, Z. Si, P. Uwer, Top quark spin correlations at hadron colliders: predictions at next-to-leading order QCD, Phys. Rev. Lett. 87 (2001) 242002.
[14] W. Bernreuther, A. Brandenburg, Z.G. Si, P. Uwer, Top quark pair production and decay at hadron colliders, Nucl. Phys. 690 (2004) 81.
[15] W. Bernreuther, Z.-G. Si, private communications, 2014.
[16] V.M. Abazov, et al., D0 Collaboration, Evidence for spin correlation in $t\bar{t}$ production, Phys. Rev. Lett. 108 (2012) 032004.
[17] T. Aaltonen, et al., CDF Collaboration, Measurement of $t\bar{t}$ spin correlation in $p\bar{p}$ collisions using the CDF II detector at the Tevatron, Phys. Rev. D 83 (2011) 031104.
[18] V.M. Abazov, et al., D0 Collaboration, Measurement of spin correlation in $t\bar{t}$ production using dilepton final states, Phys. Lett. B 702 (2011) 16.
[19] G. Aad, et al., ATLAS Collaboration, Observation of spin correlation in $t\bar{t}$ events from pp collisions at $\sqrt{s} = 7$ TeV using the ATLAS detector, Phys. Rev. Lett. 108 (2012) 212001.
[20] G. Aad, et al., ATLAS Collaboration, Measurements of spin correlation in top–antitop quark events from proton–proton collisions at $\sqrt{s} = 7$ TeV using the ATLAS detector, Phys. Rev. D 90 (2014) 112016.
[21] G. Aad, et al., ATLAS Collaboration, Measurement of the correlations between the polar angles of leptons from top quark decays in the helicity basis at $\sqrt{s} = 7$ TeV using the ATLAS detector, Phys. Rev. D 93 (1) (2016) 012002.
[22] S. Chatrchyan, et al., CMS Collaboration, Measurements of $t\bar{t}$ spin correlations and top-quark polarization using dilepton final states in pp collisions at $\sqrt{s} = 7$ TeV, Phys. Rev. Lett. 112 (2014) 182001.
[23] G. Aad, et al., ATLAS Collaboration, Measurement of spin correlation in top–antitop quark events and search for top squark pair production in pp collisions at $\sqrt{s} = 8$ TeV using the ATLAS detector, Phys. Rev. Lett. 114 (2015) 142001.
[24] V. Khachatryan, et al., CMS Collaboration, Measurement of spin correlations in $t\bar{t}$ production using the matrix element method in the muon+jets final state in pp collisions at $\sqrt{s} = 8$ TeV, Phys. Lett. B (2015), submitted for publication, arXiv:1511.06170.
[25] G. Mahlon, S.J. Parke, Spin correlation effects in top quark pair production at the LHC, Phys. Rev. D 81 (2010) 074024.
[26] V.M. Abazov, et al., D0 Collaboration, The upgraded D0 detector, Nucl. Instrum. Methods Phys. Res., Sect. A, Accel. Spectrom. Detect. Assoc. Equip. 565 (2006) 463.
[27] V.M. Abazov, et al., The muon system of the run II D0 detector, Nucl. Instrum. Methods Phys. Res., Sect. A, Accel. Spectrom. Detect. Assoc. Equip. 552 (2005) 372.
[28] M. Abolins, et al., Design and implementation of the new D0 level-1 calorimeter trigger, Nucl. Instrum. Methods Phys. Res., Sect. A, Accel. Spectrom. Detect. Assoc. Equip. 584 (2008) 75.
[29] R. Angstadt, et al., D0 Collaboration, The layer 0 inner silicon detector of the D0 experiment, Nucl. Instrum. Methods Phys. Res., Sect. A, Accel. Spectrom. Detect. Assoc. Equip. 622 (2010) 298.
[30] S. Ahmed, et al., D0 Collaboration, The D0 silicon microstrip tracker, Nucl. Instrum. Methods Phys. Res., Sect. A, Accel. Spectrom. Detect. Assoc. Equip. 634 (2011) 8.
[31] B. Casey, et al., The D0 run IIb luminosity measurement, Nucl. Instrum. Methods Phys. Res., Sect. A, Accel. Spectrom. Detect. Assoc. Equip. 698 (2013) 208.
[32] V. Bezzubov, et al., The performance and long term stability of the D0 run II forward muon scintillation counters, Nucl. Instrum. Methods Phys. Res., Sect. A, Accel. Spectrom. Detect. Assoc. Equip. 753 (2014) 105.

[33] V.M. Abazov, et al., D0 Collaboration, Electron and photon identification in the D0 experiment, Nucl. Instrum. Methods Phys. Res., Sect. A, Accel. Spectrom. Detect. Assoc. Equip. 750 (2014) 78.
[34] V.M. Abazov, et al., D0 Collaboration, Muon reconstruction and identification with the run II D0 detector, Nucl. Instrum. Methods Phys. Res., Sect. A, Accel. Spectrom. Detect. Assoc. Equip. 737 (2014) 281.
[35] G.C. Blazey, et al., in: U. Baur, R.K. Ellis, D. Zeppenfeld (Eds.), Proceedings of the Workshop on QCD and Weak Boson Physics in Run II, 2000, pp. 47–77, arXiv:hep-ex/0005012.
[36] V.M. Abazov, et al., D0 Collaboration, Jet energy scale determination in the D0 experiment, Nucl. Instrum. Methods Phys. Res., Sect. A, Accel. Spectrom. Detect. Assoc. Equip. 763 (2014) 442.
[37] V.M. Abazov, et al., D0 Collaboration, Improved b quark jet identification at the D0 experiment, Nucl. Instrum. Methods Phys. Res., Sect. A, Accel. Spectrom. Detect. Assoc. Equip. 763 (2014) 290.
[38] V.M. Abazov, et al., D0 Collaboration, Measurement of the asymmetry in angular distributions of leptons produced in dilepton $t\bar{t}$ final states in $p\bar{p}$ collisions at $\sqrt{s} = 1.96$ TeV, Phys. Rev. D 88 (2013) 112002.
[39] V.M. Abazov, et al., D0 Collaboration, Measurement of differential $t\bar{t}$ production cross sections in $p\bar{p}$ collisions, Phys. Rev. D 90 (2014) 092006.
[40] S. Frixione, B.R. Webber, Matching NLO QCD computations and parton shower simulations, J. High Energy Phys. 06 (2002) 029.
[41] S. Frixione, B.R. Webber, The MC@NLO 3.4 event generator, arXiv:0812.0770, 2008.
[42] G. Corcella, et al., HERWIG 6.5: an event generator for hadron emission reactions with interfering gluons (including supersymmetric processes), J. High Energy Phys. 01 (2001) 010.
[43] J. Pumplin, et al., New generation of parton distributions with uncertainties from global QCD analysis, J. High Energy Phys. 07 (2002) 012.
[44] P.M. Nadolsky, et al., Implications of CTEQ global analysis for collider observables, Phys. Rev. D 78 (2008) 013004.
[45] R. Brun, F. Carminati, Geant: detector description and simulation tool, CERN Program Library Long Writeup W5013, 1993, unpublished.
[46] M.L. Mangano, M. Moretti, F. Piccinini, R. Pittau, A.D. Polosa, ALPGEN, a generator for hard multiparton processes in hadronic collisions, J. High Energy Phys. 07 (2003) 001.
[47] T. Sjöstrand, S. Mrenna, P.Z. Skands, PYTHIA 6.4 physics and manual, J. High Energy Phys. 05 (2006) 026.
[48] T. Affolder, et al., CDF Collaboration, Charged jet evolution and the underlying event in $p\bar{p}$ collisions at 1.8 TeV, Phys. Rev. D 65 (2002) 092002.
[49] S. Moch, P. Uwer, Theoretical status and prospects for top-quark pair production at hadron colliders, Phys. Rev. D 78 (2008) 034003.
[50] V.M. Abazov, et al., D0 Collaboration, Measurement of spin correlation in $t\bar{t}$ production using a matrix element approach, Phys. Rev. Lett. 107 (2011) 032001.
[51] K. Melnikov, M. Schulze, Top quark spin correlations at the Tevatron and the LHC, Phys. Lett. B 700 (2011) 17.
[52] G.J. Feldman, R.D. Cousins, A unified approach to the classical statistical analysis of small signals, Phys. Rev. D 57 (1998) 3873.
[53] A. Brandenburg, Z.G. Si, P. Uwer, QCD-corrected spin analysing power of jets in decays of polarized top quarks, Phys. Lett. B 539 (2002) 235.
[54] P. Nason, S. Dawson, R.K. Ellis, The total cross-section for the production of heavy quarks in hadronic collisions, Nucl. Phys. 303 (1988) 607.
[55] M. Mangano, F. Stefano, private communications, 2014.